Available online at www.sciencedirect.com

ScienceDirect

Energy Procedia 69 (2015) 1296 – 1305

Energy Procedia

International Conference on Concentrating Solar Power and Chemical Energy Systems, SolarPACES 2014

Evaluation of glare at the Ivanpah Solar Electric Generating System

C. K. Ho,[a,]* C. A. Sims,[b] and J. M. Christian[a]

[a]*Sandia National Laboratories, P.O. Box 5800, Albuquerque, NM 87185, USA*
[b]*Sims Industries, LLC, 85 Poinciana Dr., Dayton, OH 45459, USA*

Abstract

The Ivanpah Solar Electric Generating System (ISEGS), located on I-15 about 40 miles (60 km) south of Las Vegas, NV, consists of three power towers 459 ft (140 m) tall and over 170,000 reflective heliostats with a rated capacity of 390 MW. Reports of glare from the plant have been submitted by pilots and air traffic controllers and recorded by the Aviation Safety Reporting System and the California Energy Commission since 2013. Aerial and ground-based surveys of the glare were conducted in April, 2014, to identify the cause and to quantify the irradiance and potential ocular impacts of the glare. Results showed that the intense glare viewed from the airspace above ISEGS was caused by heliostats in standby mode that were aimed to the side of the receiver. Evaluation of the glare showed that the retinal irradiance and subtended source angle of the glare from the heliostats in standby were sufficient to cause significant ocular impact (potential for after-image) up to a distance of ~6 miles (10 km), but the values were below the threshold for permanent eye damage. Glare from the receivers had a low potential for after-image at all ground-based monitoring locations outside of the site boundaries. A Letter to Airmen has been issued by the Federal Aviation Administration to notify pilots of the potential glare hazards. Additional measures to mitigate the potential impacts of glare from ISGES are also presented and discussed.

Peer review by the scientific conference committee of SolarPACES 2014 under responsibility of PSE AG

Keywords: Concentrating solar power, glare, glint, heliostats, standby, Ivanpah solar

* Corresponding author. Tel.: 1-505-844-2384; fax: 1-505-845-3366.
E-mail address: ckho@sandia.gov

Peer review by the scientific conference committee of SolarPACES 2014 under responsibility of PSE AG
doi:10.1016/j.egypro.2015.03.150

1. Introduction

The Ivanpah Solar Electric Generating System (ISEGS) consists of three power towers generating 392 MW on 14.2 km^2 (3500 acres) of public desert land in southern California. Over 170,000 heliostats with 2.6 million square meters of mirrors reflect and concentrate sunlight toward the receivers at the top of the 140 m (459 ft) towers that produce steam for the power cycle (Figure 1).

Fig. 1. Illuminated receivers at ISEGS, Feb. 2014 (source: Wikipedia)

Reports of glare from pilots and air traffic controllers have been docketed by the California Energy Commission (CEC) [1]. One pilot stated the following as they departed from Boulder City airport and climbed southwest over ISEGS, "At its brightest neither the pilot nor co-pilot could look in that direction due to the intense brightness. From the pilot's seat of my aircraft the brightness was like looking into the sun and it filled about 1/3 of the co-pilots front windshield. In my opinion the reflection from these mirrors was a hazard to flight because for a brief time I could not scan the sky in that direction to look for other aircraft." An air-traffic controller stated, "Daily, during the late morning and early afternoon hours we get complaints from pilots of aircraft flying from the northeast to the southwest about the brightness of this solar farm." These complaints were recorded in August 2013 in NASA's Aviation Safety Reporting System and docketed with ISEGS compliance proceedings (07-AFC-05C) on March 10, 2014. The Federal Aviation Administration (FAA) reported that in May 2014, nearly 12,000 flights were recorded passing within a 15 nautical mile (28 km) radius of ISEGS [2].

The Heliostat Positioning Plan and the Power Tower Luminance Monitoring Plan [3, 4] define glare and monitoring requirements at ISEGS as agreed upon between the CEC and the operators/developers of ISEGS (NRG/Brightsource). Both aerial and ground-based surveys of glare events and their potential impacts were required. The objective of this work was to conduct aerial and ground-based surveys of the glare at ISEGS to understand the causes, impact, and possible mitigation measures. Models of the specular (reflections from mirrors) and diffuse (reflections from the receiver) glare are presented and compared to the empirical results. The causes of the glare are described, and the irradiance and potential ocular impacts are quantified as a function of distance from the glare source. Measures to mitigate the impacts of glare are discussed.

2. Description of potential glare hazards

Impacts of glint and glare on eyesight can include discomfort, disability, veiling effects, after-image and retinal burn [5-8]. Prolonged exposure to "discomfort glare" may lead to headaches and other physiological impacts, whereas "disability glare" immediately reduces visual performance. Disability glare can include after-image effects, flash blindness and veiling, such as that caused by solar glare on a windshield that might mask pedestrians, vehicles, or aircraft. Retinal burn can occur with exposure to lasers or concentrated sunlight.

Ho et al. [9] developed irradiance models and summarized the potential impacts to eyesight as a function of retinal irradiance (the solar flux entering the eye and reaching the retina) and subtended source angle (size of glare source divided by distance). Figure 2 shows the resulting "Ocular Hazard Plot" with three regions: (1) potential for

permanent eye damage (retinal burn), (2) potential for temporary after-image, and (3) low potential for temporary after-image. If the retinal irradiance or subtended angle is sufficiently large, permanent eye damage from retinal burn may occur (e.g., from concentrating mirrors). Below the retinal burn threshold, a region exists where a sufficiently high retinal irradiance may cause a temporary after-image, which is caused by bleaching (oversaturation) of the retinal visual pigments. The size and impact of the after-image in the field of view depends on the size of the subtended source angle. For a given retinal irradiance, smaller source angles yield smaller after-images, and the potential impact is less. Sufficiently low retinal irradiances and/or subtended angles of the glare source have a low potential for after-image and ocular impacts.

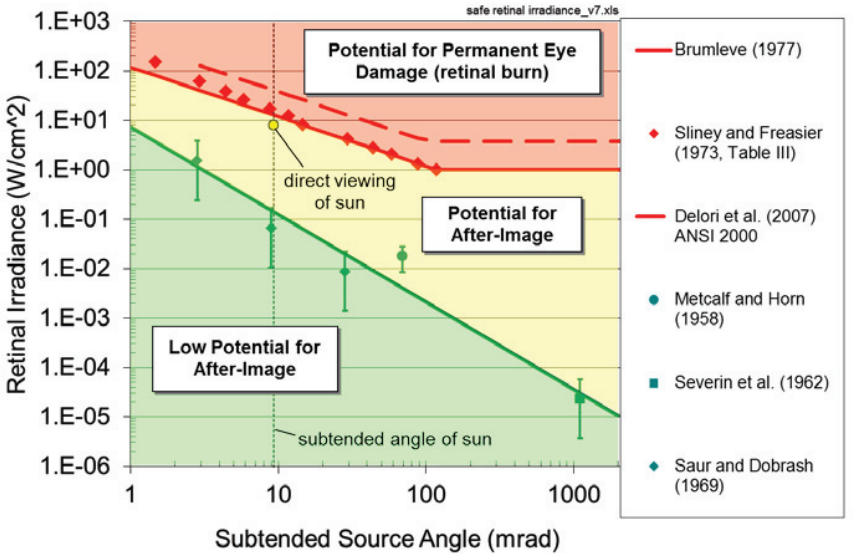

Fig. 2. Potential ocular impacts of retinal irradiance as a function of subtended source angle [9]. Note: 1 watt yields approximately 100 lumens of visible light in the solar spectrum.

A number of factors can affect both the intensity and perceived impact of glare: direct normal irradiance (DNI), reflectance, distance, size of the reflecting surfaces, and human factors. The DNI is the amount of solar irradiance striking a surface perpendicular to the sun's rays. A typical clear sunny day may yield a DNI of ~1,000 watts per square meter at solar noon, with lower values in the mornings and evenings. The DNI provides the starting "strength" of the solar glare source, which can then be reduced by the reflectance of the mirror or receiver. The reflected light can be characterized as a combination of specular (mirror-like) and diffuse (scattered) reflections. Smooth surfaces such as mirrors and smooth glass produce more specular reflections with greater intensity and tighter beams (larger retinal irradiances and smaller subtended angles used in Figure 2), while solar receivers produce more diffuse reflections with lower solar intensities but greater subtended angles. Typically, specular reflections pose a greater risk for ocular hazards.

The distance between the observer and the glare source can impact both the retinal irradiance and subtended source angle. Atmospheric attenuation caused by particulates or humidity in the air will reduce the retinal irradiance with increasing distance.[†] In addition, for a fixed size of the glare source, larger distances will typically yield smaller subtended angles of the glare source. Finally, human factors such as ocular properties (pupil size, eye focal length, ocular transmittance) and light sensitivity will affect the retinal irradiance, subtended angle and perceived impact of the glare. Typical ocular properties for daylight adjusted eyes are provided in Ho et al. [9].

[†] Without atmospheric attenuation, the retinal irradiance [W/m^2] is independent of distance since the power entering the eye (numerator) and exposed retinal area (denominator) decrease at the same rate with increasing distance.

3. Aerial glare surveys

3.1. Approach

On April 24, 2014, aerial surveys of the glare at ISEGS were performed via helicopter (R-44 rented from Airworks LV in Las Vegas, NV). A Nikon D90 camera was used with Tiffen neutral density filters to record images of the glare during the aerial flyovers. Photographs of the glare were processed using the PHLUX method [10, 11] to quantify the irradiance and potential ocular impacts as a function of distance from the glare source. Figure 3 shows the locations of the aerial photographs that were taken to quantify the glare and potential ocular impacts at distances ranging from ~1 – 20 miles (1.6 – 32 km). Video of the glare was also recorded around the entire site (Units 1, 2, and 3).

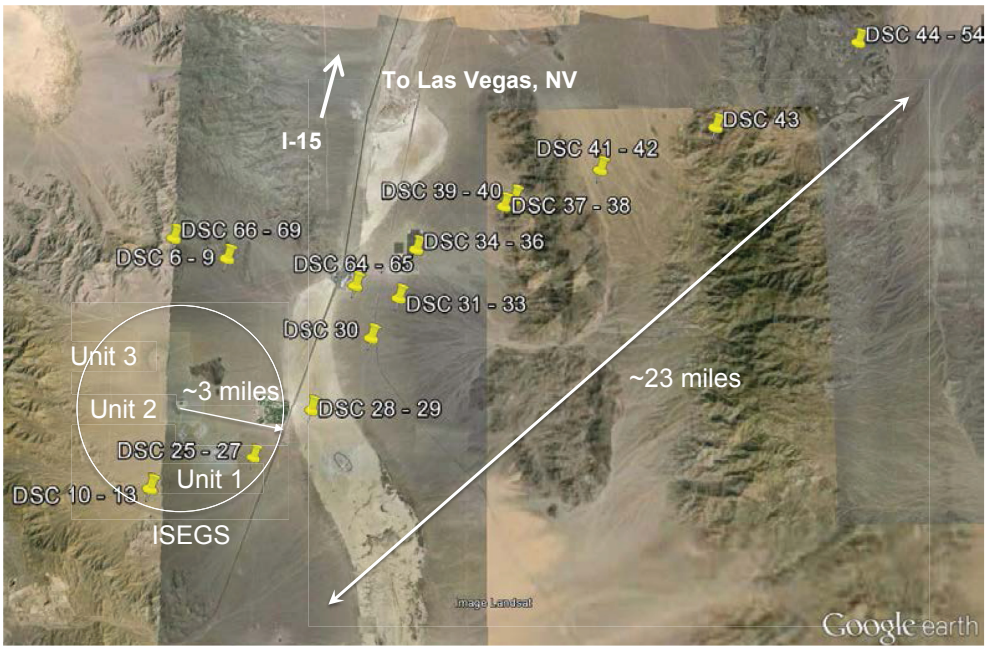

Fig. 3. Locations of aerial photos that were taken of the glare visible at ISEGS (located within the circle), April 24, 2014. The "DSC" labels refer to the photo numbers in Table 1.

3.2. Results

Figure 4 shows photos of glare observed at various locations around ISEGS taken from the helicopter. The glare was bright and visible in all radial directions from ISEGS out to distances greater than 20 miles (32 km) from the site. Filtered images of the glare (Figure 4) reveal that the source of the intense glare is from heliostats in standby mode in which they are aimed at points next to the receiver rather than on the receiver itself. The diffuse reflections from the receiver produce irradiances that are much lower than the specular reflections from the heliostat. In fact, filtered images of the glare (Figure 4) show that the receiver appears dark relative to the glare from the heliostats. Glare from Unit 1 that was visible from a particular observation point was caused by multiple heliostats on both sides of the receiver. Typically, heliostats in standby mode are aimed toward a ring of points around the receiver, with each heliostat along a radial line aimed toward a single point next to the receiver. The use of two standby points on either side of the receiver for "pairs" of heliostats along a radial line or zone from Unit 1 was confirmed during personal communication with Brightsource operators. Although glare from standby heliostats at Units 2 and 3 was also visible, it was not clear if those units implemented "pairs" of heliostats aimed toward both sides of the

receiver. In all cases, as the azimuthal position of the heliostats revolve around the tower, the standby aim points also revolve around the receiver, creating a ring of aim points (see Section 3.3).

The elevation at which glare was observed ranged from ~5000' – 8400' (1.5 – 2.6 km) above mean sea level, depending on the distance from the site. The ground elevation at ISEGS ranges from ~2800' – 3300' (850 – 1000 m) above mean sea level. At a particular distance, higher elevations will yield glare from heliostats closer to the tower while lower elevations will yield glare from heliostats further from the tower. Section 3.3 demonstrates that a toroid of glare is formed in the airspace above ISEGS from heliostats in standby mode. The region for potential glare is fairly ubiquitous, but regions where glare might not be observed include high elevations directly above the receiver and low elevations at distances far from the site. However, because of the presence of the three separate units, glare will likely be visible in the airspace around ISEGS at all locations whenever the site is in view and when heliostats are in standby mode.

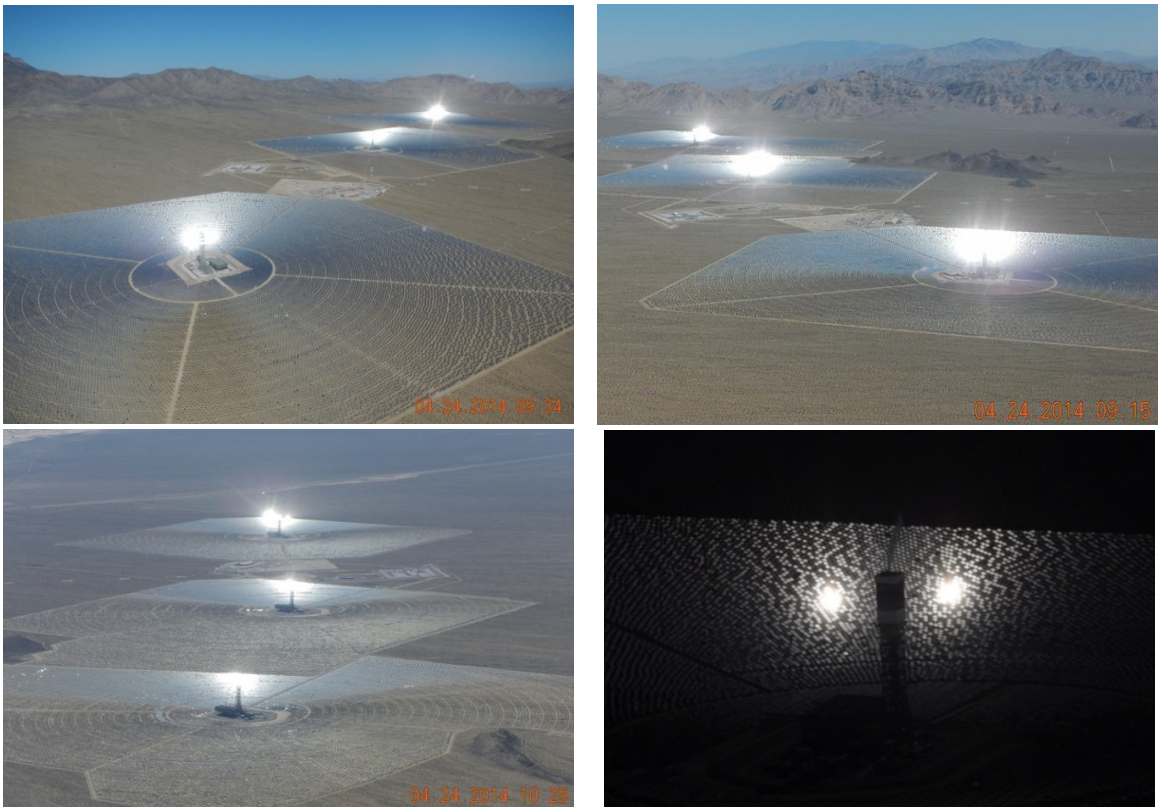

Fig. 4. Photos of observed glare at various locations around ISEGS during aerial survey, April 24, 2014, 9:15 – 10:30 AM PDT.

Table 1 summarizes the irradiance and ocular impact of the glare at various aerial locations around ISEGS. The peak retinal irradiance and subtended angle from a single heliostat image was determined from the photographs of glare using the PHLUX method [10, 11]. The subtended angle of the entire glare source in the photograph was calculated by assuming the entire glare from the visible heliostats formed a single contiguous glare source. The total subtended angle, which is proportional to the square root of the visible glare area, is then calculated as the product of the subtended angle of the single heliostat image and the square root of the total number of visible heliostat images in the photograph. The DNI ranged from 790 – 860 W/m^2 during the survey, with most of the photos taken at a DNI of 850 W/m^2. Most of the photos that were quantified using the PHLUX method were taken of the glare from Unit 1 for consistency. A few photos were taken of Unit 3 and processed in Table 1, but no helicopter images were

quantified of Unit 2. Units 1 and 3 appeared to produce the most amount of glare during the survey up to distances of ~20 miles (32 km).

Results show that the retinal irradiance and subtended source angle of the glare were sufficiently large to produce ocular impacts (potential for after-image) out to a distance of 6 miles (10 km). The retinal irradiance is highest (~6 W/cm^2) at locations close to the site, but atmospheric attenuation reduces the irradiance at longer distances. The subtended angle also decreases with increasing distance, and this reduces the potential ocular impact as shown in the Ocular Hazard Plot in Figure 2. Section 3.3 presents models that show that as the observer distance increases, the number of visible glare-producing heliostats decreases at any particular location. At distances greater than ~6 miles (10 km), a low potential for after-image exists from the heliostat glare as a result of the reduced retinal irradiance and subtended angles. It should be noted that two of the authors who were in the helicopter qualitatively confirmed these results after observing the glare. The pilot acknowledged that the glare was very bright, but he also stated that it did not impair his flying ability since he was aware of the glare and avoided looking in that direction when flying over ISEGS.

Table 1. Processed data from photos of glare at ISEGS (4/24/14).

Image	Tower Unit	Approximate Distance to Glare (miles (km))	Peak Retinal Irradiance (W/cm^2)	Total Subtended Glare Angle* (mrad)	Ocular Impact
DSC 26	1	1 (1.6)	6.39	4.13	Potential for Temporary After-Image
DSC 28	1 (left aim point)	3 (4.8)	5.10	1.60	Potential for Temporary After-Image
DSC 28	1 (right aim point)	3 (4.8)	2.81	1.90	Potential for Temporary After-Image
DSC 08	3	4 (6.4)	2.12	3.64	Potential for Temporary After-Image
DSC 08	3	4 (6.4)	1.98	4.03	Potential for Temporary After-Image
DSC 30	1	6 (9.7)	2.15	3.47	Potential for Temporary After-Image
DSC 65	1	6 (9.7)	4.25	1.60	Potential for Temporary After-Image
DSC 32	1	7 (11)	5.45	1.06	Low Potential for After-Image
DSC 34	1	11 (18)	5.29	0.586	Low Potential for After-Image
DSC 41	3	15 (24)	1.39	0.760	Low Potential for After-Image
DSC 53	3	23 (37)	0.112	0.541	Low Potential for After-Image

*Subtended angle is assumed proportional to the square root of the number (area) of visible heliostats producing glare.

3.3. Modeling of standby heliostats

Figure 5 shows a simulation of the illuminated region around the tower when the heliostats are in a standby mode (i.e., aimed at a ring of locations next to the receiver, creating a large toroid of illumination in the airspace above the tower). To better understand this illustration, one can imagine that the heliostat field forms a “wheel” around the base of the tower. Heliostats along each “spoke” of the wheel are aimed to the same point next to the receiver. Different spokes of heliostats will have different aim points that form a ring around the receiver. If all the heliostats are positioned in standby mode in this fashion, a toroid of glare will be formed that is defined by the radius of the heliostat field (heliostats closest to the tower will define the most vertical rays of reflected light, and the heliostats furthest from the tower will define the most horizontal rays of reflected light). A band free from glare exists at an elevation near the receiver, and the left photograph in Figure 5 illustrates similar behavior. The bright spot to the right of the receiver in the photograph is caused by accumulated particulates in the air above the air cooled condenser, which draws ambient air through a series of large fans near the base of the tower (the visible building next to the tower).

The model assumes specular reflections from standby heliostats aimed at a fixed position next to the receiver such that the maximum glare spot size can be represented by a parabolic reflector with a diameter equal to the radius of the heliostat field (distance between the outer and inner rows of heliostats). The predicted number of visible

heliostats was relatively insensitive to the assumed diameter of the parabolic reflector, but it was more sensitive to the distance between the heliostat and aim point, as well as the observer location if it was near the aim point. Assuming a direct normal irradiance of 1000 W/m^2, a heliostat reflectance of 0.93, and typical ocular parameters [9], the model predicts a potential for after-image out to ~6 miles (~10 km), similar to the aerial surveys. It should be noted that a single 15 m^2 heliostat is predicted to produce a potential for after-image up to a distance of 2.5 miles (~4 km).

A Tower Illuminance Model (TIM) is being developed at Sandia that will allow simulated "flyovers" of power towers with prescribed height, diameter, heliostat field size, reflectance, and other relevant parameters to determine the irradiance and potential ocular impact at any location in the airspace above the site.

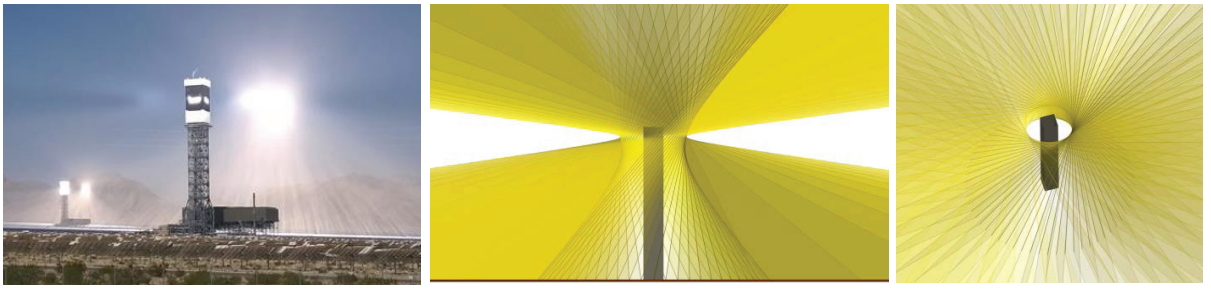

Fig. 5. Photo (left; Ryan Goerl, NRG) and model (middle and right) of illuminance from heliostats aimed at a standby point near the top of the tower, forming a toroid of glare in the airspace.

4. Ground-based glare surveys

4.1. Approach

Similar to the aerial surveys, photographs were taken using a D90 camera and Tiffen neutral density filters from ground-based locations around the site and along I-15. The PHLUX method [10, 11] was used to quantify the irradiance and potential ocular impacts at various locations. In addition, videos were taken while driving both southbound and northbound along I-15 (Figure 6).

Fig. 6. Photograph of illuminated receivers at Units 2 and 3 while heading southbound along I-15.

4.2. Results

Figure 7 shows an example of a processed image of the glare from the Unit 1 receiver as viewed from I-15 approximately 1.5 miles (2.4 km) away. The processed image of the photograph of the receiver shows bright spots on the white heat shields above and below the receiver, which is black and less reflective.

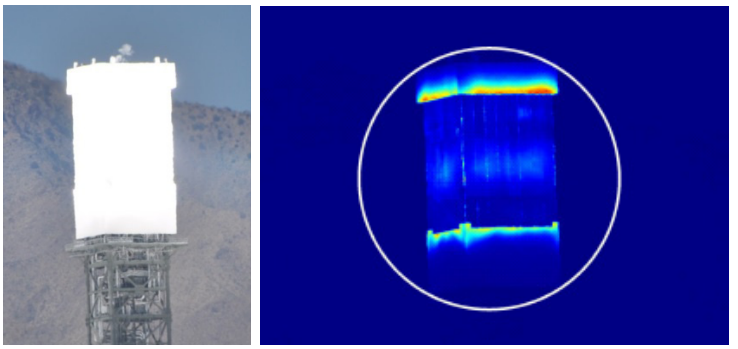

Fig. 7. Photo (left) and measured irradiance profile (right) of unit 1 receiver from I-15 (~1.5 miles away) at ~1:00 PM PDT, 4/24/14.

The retinal irradiance from the receiver glare was approximately 0.001 W/cm^2 (much lower than the 6 W/cm^2 peak retinal irradiance received from standby heliostats), and the subtended angle of the glare was nearly 20 mrad (much greater than the maximum subtended angle of 4 mrad from the standby heliostats at a mile away). The combined effect of the retinal irradiance and subtended angle of the receiver glare resulted in a "low potential for after-image." After viewing the glare from the receiver, two of the authors noted that, while bright, no prolonged after-image was observed. In addition, during the drive-by surveys along I-15, the driver did not notice any visual impairment, primarily because the glare source was off to the side and not within the driver's line of sight.

Figure 8 shows a photograph of the Unit 3 receiver viewed from I-15, along with a "rogue" heliostat that is reflecting the sunlight toward I-15. Occasionally, the authors observed glare from individual heliostats visible along the highway, and photographs were taken. When processed, the image of the glare from an individual heliostat had a "low potential for after-image", but the retinal irradiance and subtended angle were close to the ocular threshold for after-image. While these rogue heliostats may pose an ocular impact while stationary, the authors noted that while driving, the glare was only momentary and off to the side. Therefore, the ocular impact from individual rogue heliostats was not perceived to be significant.

4.3. Modeling of receivers

Ho et al. [9] provides models to determine the irradiance and potential ocular impacts of glare from diffuse reflections from receivers. Assuming a direct normal irradiance value of 0.1 W/cm^2, receiver reflectance of 0.05, concentration ratio of 400, and default ocular parameters [9], the model predicts a retinal irradiance of ~0.003 W/cm^2 and a subtended angle of 16 mrad from a distance of 1.5 miles (2.4 km) away (assuming the full height of the receiver (22 m) plus shielding (~16 m). These results are consistent with the observations reported in Section 4.2 and yield a low potential for after-image.

5. Mitigation measures

5.1. Letter to Airmen

A Letter to Airmen notifying pilots of potential glare from ISEGS was issued by the Federal Aviation Administration on May 5, 2014. The letter was intended to provide advanced notice to pilots flying over the ISEGS

site so that they are aware of the potential glare hazards as they approach the site and can take protective actions, as appropriate.

Fig. 8. Photograph of Unit 3 receiver and "rogue" heliostat from I-15 (~3 miles away).

5.2. Modification of heliostat standby positions

Brightsource and NRG are also investigating new strategies and algorithms for heliostat standby positions to reduce the irradiance and number of heliostats that can reflect light to an aerial observer. Some strategies that Sandia has recommended include the following;

- Increase the number of aim points near the receiver and have adjacent heliostats point to different locations so that the number of glare-producing heliostats visible from the airspace above is minimized at all locations
- Position heliostats vertically or in other orientations that minimize glare
- Bring heliostats up to standby position at top of receiver sequentially as needed to avoid having a large number of heliostats reflecting light into the airspace above
- Incorporate a glare shield near the receiver that can serve as both the aim point for heliostats in standby mode and a preheater for the water entering the receiver

6. Summary and conclusions

Aerial and ground-based surveys have been conducted to identify the causes and potential impact of glare observed at ISEGS. These surveys satisfy, in part, monitoring requirements prescribed in the Heliostat Positioning Plan and the Power Tower Luminance and Monitoring Plan [3, 4]. Findings from the aerial and ground-based surveys are summarized as follows:

- Aerial Surveys
    - Heliostats in standby mode can cause glare to aerial observers (pilots)
    - Glare from heliostats can cause after-image at far distances (up to 6 miles (10 km) in our helicopter surveys)
    - Glare was visible from multiple heliostats in standby mode
    - Glare from Unit 1 originated from standby heliostats on both sides of the receiver during the survey on April 24, 2014

    - The glare from the illuminated receiver was small compared to the glare from the standby heliostats
- Ground Surveys
    - Drive-by surveys at three different times of the day did not reveal any ocular hazards
    - All data from receiver glare showed a low potential for after-image
    - Glare from an occasional rogue heliostat was visible from I-15, but it was not perceived to be a significant ocular hazard
- Modeling
    - Modeling of both specular reflections from heliostats and diffuse reflections from the receiver predicted retinal irradiances, subtended angles, and ocular impacts that were consistent with the results of the aerial and ground surveys

Mitigation measures that have been implemented include a Letter to Airmen that was issued on May 5, 2014, notifying pilots of potential glare at ISEGS. In addition, new strategies for positioning heliostats in standby mode are being developed and implemented to reduce the potential impacts of glare.

Acknowledgements

Sandia National Laboratories is a multi-program laboratory managed and operated by Sandia Corporation, a wholly owned subsidiary of Lockheed Martin Corporation, for the U.S. Department of Energy's National Nuclear Security Administration under contract DE-AC04-94AL85000. The United States Government retains and the publisher, by accepting the article for publication, acknowledges that the United States Government retains a non-exclusive, paid-up, irrevocable, world-wide license to publish or reproduce the published form of this manuscript, or allow others to do so, for United States Government purposes.

References

[1] California Energy Commission. Letter re Pilot Complaints of Visual Impacts from Ivanpah Solar Electric Generating System, March 10, 2014.
[2] California Energy Commission. Email Re: Request for Ivanpah Report, dated June 10, 2014, June 24, 2014.
[3] CH2MHILL. Heliostat Positioning Plan for the Ivanpah Solar Electric Generating System Eastern Mojave Desert San Bernardino County, California. Prepared for Solar Partners I, LLC; Solar Partners II, LLC; and Solar Partners VIII, LLC; 2013.
[4] CH2MHILL. Power Tower Luminance Monitoring Plan for the Ivanpah Solar Electric Generating System Eastern Mojave Desert San Bernardino County, California. Prepared for Solar Partners I, LLC; Solar Partners II, LLC; and Solar Partners VIII, LLC; 2013.
[5] Saur RL, Dobrash SM. Duration of Afterimage Disability after Viewing Simulated Sun Reflections. Applied Optics, 8(9). 1969; p. 1799-1801.
[6] Sliney DH, Freasier BC. Evaluation of Optical Radiation Hazards. Applied Optics, 12(1). 1973; p. 1-24.
[7] Nakagawara VB, Wood KJ, Montgomery RW. Natural Sunlight and Its Association to Aviation Accidents: Frequency and Prevention. DOT/FAA/AM-03/6. Civil Aerospace Medical Institute, Federal Aviation Administration. Oklahoma City, OK; 2003.
[8] Osterhaus WKE. Discomfort glare assessment and prevention for daylight applications in office environments. Solar Energy, 79(2). 2005; p. 140-158.
[9] Ho CK, Ghanbari CM, Diver RB. Methodology to Assess Potential Glint and Glare Hazards From Concentrating Solar Power Plants: Analytical Models and Experimental Validation. Journal of Solar Energy Engineering-Transactions of the Asme, 133(3). 2011.
[10] Ho CK, Khalsa SS. A Photographic Flux Mapping Method for Concentrating Solar Collectors and Receivers. Journal of Solar Energy Engineering-Transactions of the Asme, 134(4). 2012.
[11] Ho CK. Relieving a Glaring Problem, in Solar Today2013, American Solar Energy Society: Boulder, CO. p. 28 - 31.